Biochimica et Biophysica Acta 1820 (2012) 44–55

Contents lists available at SciVerse ScienceDirect

Biochimica et Biophysica Acta

journal homepage: www.elsevier.com/locate/bbagen

Phosphorylation of the arginine/serine repeats of lamin B receptor by SRPK1—Insights from molecular dynamics simulations

Diamantis Sellis [a,1], Victoria Drosou [b,1], Dimitrios Vlachakis [a], Nikolas Voukkalis [b], Thomas Giannakouros [b], Metaxia Vlassi [a,*]

[a] Laboratory of Protein Structure & Molecular Modeling, Institute of Biology, National Centre for Scientific Research "Demokritos", Agia Paraskevi, 15310, Greece
[b] Laboratory of Biochemistry, Department of Chemistry, Aristotle University of Thessaloniki, Thessaloniki, 54124, Greece

ARTICLE INFO

Article history:
Received 28 July 2011
Received in revised form 14 October 2011
Accepted 20 October 2011
Available online 26 October 2011

Keywords:
RS repeats
Lamin B receptor
Phosphorylation
SRPK1
Molecular dynamics simulations

ABSTRACT

Background: Arginine/serine (RS) repeats are found in several proteins in metazoans with a wide variety of functions, many of which are regulated by SR protein kinase 1 (SRPK1)-mediated phosphorylation. Lamin B receptor (LBR) is such a protein implicated in chromatin anchorage to the nuclear envelope.
Methods: Molecular dynamics simulations were used to investigate the conformation of two LBR peptides containing four (human-) and five (turkey-orthologue) consecutive RS dipeptides, in their unphosphorylated and phosphorylated forms and of a conserved peptide, in isolation and in complex with SRPK1. GST pull-down assays were employed to study LBR interactions.
Results: Unphosphorylated RS repeats adopt short, transient helical conformations, whereas serine phosphorylation induces Arginine-claw-like structures. The SRSRSRSPGR peptide, overlapping with the LBR RS repeats, docks into the known, acidic docking groove of SRPK1, in an extended conformation. Phosphorylation by SRPK1 is necessary for the association of LBR with histone H3.
Conclusions: The C-terminal region of the LBR RS domain constitutes a recognition platform for SRPK1, which uses the same recognition mechanism for LBR as for substrates with long RS domains. This docking may promote unfolding of the RS repeats destined to be phosphorylated. Phosphorylation induces Arginine-claw-like conformations, irrespective of the RS-repeat length, that may facilitate interactions with basic partners.
General significance: Our results shed light on the conformational preferences of an important class of repeats before and after their phosphorylation and support the idea that even short RS domains may be constituents of recognition platforms for SRPK1, thus adding to knowledge towards a full understanding of their phosphorylation mechanism.

1. Introduction

Reversible protein phosphorylation provides a major regulatory mechanism in eukaryotic cells. Even though it is the most commonly studied type of post-translational modification worldwide, the main effort of most groups is to delineate its signaling outcomes, whereas its structural consequences have not been yet well understood. The physical effects of phosphorylation have been shown to range from a change in the rate of cis/trans isomerization of a serine–proline motif after the phosphorylation of the serine residue to much larger conformational changes [[1 and references therein]. Based on the observation that amino acid compositions, sequence complexity, hydrophobicity and charge of regions adjacent to phosphorylation sites are very similar to those of intrinsically disordered proteins, it has been suggested that protein phosphorylation predominantly occurs within intrinsically disordered protein regions [2]. There is now fairly large literature on the structural consequences of phosphorylation: While there are several reports suggesting that phosphorylation results in a conformational change from a predominately unfolded state to a more ordered structure, molecular dynamics simulations in other proteins as well as experimental data indicate that order-to-disorder transition may also follow the phosphorylation event (for a review see Ref. [3]).

Arginine/Serine (RS)-rich domains were initially considered a new class of targeting signals, directing localization of splicing-associated proteins in nuclear speckles [4]. In the following years several reports documented the existence of a large number of RS-repeat-containing proteins in metazoans with functions not only related to pre-mRNA processing, but associated with chromatin structure, transcription by RNA polymerase II, germ cell development, osmotic regulation, cell cycle and cell structure (for review see Refs. [5,6]). RS domains have been implicated both in protein interactions with other RS

* Corresponding author. Tel.: +30 210 6503574; fax: +30 210 6511767.
E-mail address: meta@bio.demokritos.gr (M. Vlassi).
[1] These authors contributed equally to this work.

0304-4165/$ – see front matter © 2011 Elsevier B.V. All rights reserved.
doi:10.1016/j.bbagen.2011.10.010

domain-containing proteins as well as in nonsequence specific interactions with RNA molecules [7–10].

SR protein kinase 1 (SRPK1) has been shown to be the main kinase that phosphorylates RS domains [6,11]. Phosphorylation by SRPK1 is mediated by recognition of conserved docking motifs in its substrates [12–14]. The docking motifs are generally rich in basic residues, conforming to the consensus sequence, R-x-R/K-x-x-x-R [12] and bind to an acidic groove of SRPK1, which is located far from the active site [12–14]. Although a common mechanism has been proposed to be used by the kinase to recognize its substrates, the mechanism of phosphorylation seems to be substrate-dependent [14].

Despite their abundance and importance and although several, both theoretical as well as experimental studies (circular dichroism and crystallographic data on the free and SRPK1-bound forms, respectively) exist on the RS domain of the human splicing factor, ASF/SF2 [13,15], the conformation of the RS repeats in their free form, as well as the specific conformational changes induced upon phosphorylation of their serine residues, remain rather elusive. To address these issues, in this study we applied molecular dynamics (MD) simulations on a number of unphosphorylated and phosphorylated peptides of the significantly shorter RS domain of lamin B receptor (LBR), which consists of four ($(RS)_4$; human orthologue) or five consecutive RS dipeptides ($(RS)_5$; chicken orthologue). LBR is an integral protein of the inner nuclear membrane consisting of a hydrophilic N-terminal domain, protruding into the nucleoplasm, where the RS repeats are located, eight hydrophobic segments that are predicted to span the membrane, and a hydrophilic C-terminal tail [16,17]. LBR is one of the key factors that has been implicated in chromatin anchorage to the nuclear envelope [18]. SRPK1 has been found to phosphorylate any one of the serine residues of the RS repeats of turkey LBR as long as those RS dipeptides are followed by the downstream flanking sequence, PGRPAKG [19,20].

For our MD simulations, we first tested various force fields and found that, only the Amber99SB force field [21] was able to produce results in agreement with circular dichroism (CD) data on the RS domain of ASF/SF2 [13]. Our Amber99SB MD simulations revealed that, in their free form, the unphosphorylated RS repeats of LBR follow flexible structures consisting of short, transient helical elements including only two consecutive RS dipeptides at the time, instead of a stable α-helical structure extending thought their length, which has been proposed earlier by a similar study on eight consecutive RS dipeptides of the much longer RS domain of ASF/SF2 [15]. On the other hand, our MD simulations on the phosphorylated $(RS^p)_4$ peptide showed that serine phosphorylation of the RS repeats induces the formation of an Arg-claw-like structure, exposing phosphate groups to the periphery, very much alike the one found in the case of the phosphorylated RS domain of ASF/SF2 [15], suggesting that the tendency to form Arg-claw-like structures, that may serve as molecular recognition elements of basic partners, is a general property of phosphorylated RS repeats, irrespective of their length. In this respect, we demonstrated that the interaction of LBR with its basic partner, histone H3 is possible only after phopshorylation of LBR by SRPK1.

Furthermore, using molecular dynamics simulations together with biochemical data and prior knowledge, we provide evidence that the highly conserved in all LBRs RSRSPGR peptide, overlapping with the RS repeats, may serve as a docking motif for SRPK1. A possible role of this docking interaction in the unfolding of adjacent RS repeats of LBR prior to their phosphorylation is suggested by our MD simulations. Moreover, our MD simulations suggest that SRPK1 uses the same, distal to the active site, acidic docking groove to recognize the LBR motif, as its other substrates. However, the short length of the LBR RS repeats as well as their overlapping with the docking motif, imply that SRPK1 must use for LBR a different substrate feeding mechanism than the one proposed for the phosphorylation of proteins with long RS domains [11]. Finally, our results suggest for the first time that the RS repeats of both short and long RS domains may be a constituent of the docking motif recognized by SRPK1.

2. Materials and methods

2.1. Sequence alignment

The GeneDoc multiple sequence alignment editor and shading utility [22] was used to edit multiple alignments of LBR sequences.

2.2. Molecular modeling

2.2.1. Construction of initial structures

The starting peptide conformations (ideal extended-strand: $\varphi = -120°$, $\psi = 120°$) for the implicit MD simulations, were obtained using the Swiss-pdb viewer [23]. Their Ace-, Nme-blocked termini were constructed based on Ala residues. The same program was used to construct the 3D-model of the Ac-S^{78}RSRSRSPGR^{87}-NHMe peptide of turkey LBR (peptide R2′) in complex to SRPK1. The crystal structure of SRPK1 complexed to a substrate 10-mer peptide, SYGRSRSRSR, from ASF/SF2 protein (RCSB code: 3BEG) [13] was used as a template for this purpose. The *Mutate* tool of the Swiss-pdb viewer was applied on the template ASF/SF2 peptide to obtain the coordinates of the bound to SRPK1 R2′ peptide. The 3D-model of the peptide alone, in its SRPK1 bound conformation, was used as the initial structure for the explicit MD simulation of the R2′ peptide in isolation, whereas the 3D-model of the peptide in complex with the "docking domain" of SRPK1 (aa: 172–216 and 482–655) was utilized to simulate the peptide in the presence of SRPK1.

2.2.2. Molecular dynamics simulations

Molecular dynamics (MD) simulations were performed using the GROMACS4 (v. 4.5.3) software package [24] through a new version of the Gromita GUI, we have developed previously [25].

As a starting point, implicit Generalized Born (GB) solvation was used in the MD simulations because implicit solvation models offer significant computational savings when an extensive sampling of conformations is required, while yielding an accurate treatment of solvation. The MD simulations in implicit solvation were carried out for 200 ns at 300 K by using the GB/SA solvation and the Still method for calculating the Born radii [26]. The Ac-$(RS)_4$-NHMe and Ac-$(RS)_5$-NHMe peptides in an ideal extended-strand conformation, were used as the initial structures, for the unphosphorylated case. The peptides were capped with ACE and NME blocking groups to minimize the possibility of salt-bridge traps resulting from the charged termini. The all-atom AMBER03 [27] and AMBER99SB [21] force fields, as implemented in GROMACS4, were used for this purpose. The AMBER03 force field was used first, for comparison with a similar study on the $(RS)_8$ peptide of ASF/SF2 [15], while the AMBER99SB force field was used as it has been shown to provide better balance of secondary structure elements [21]. An additional set of 200 ns MD simulation using the AMBER96 force field in combination with the OBC (II) implicit solvent model was also carried out for the unphosphorylated $(RS)_4$ peptide. This combination was tested as it has been shown to provide reliable structure predictions for various peptides [28]. The surface tension parameter for the non-polar solvation term was set to the default values of 0.0049 and 0.0054 kcal/mol/Å^2 for the Still and OBC methods, respectively. For the phosphorylated form, a 200 ns MD simulation with implicit solvation was carried out for the fully phosphorylated human peptide, Ac-$(RS^p)_4$-NHMe, starting from an ideal extended-strand conformation. The AMBER99SB force field and the Amber S2P parameters for the phosphoserines [29] (adapted from the Bryce R, AMBER Parameter Database, http://pharmacy.man.ac.uk/amber) were used in this simulation.

The MD simulations in explicit water were carried out using periodic cubic boxes of TIP3P water molecules [30] to solvate the peptides

in their free forms, whereas a periodic triclinic box of TIP3P water molecules, extending 0.85 nm from protein atoms, was used in the case of the SRPK1:R2′ peptide complex. Periodic boundaries were applied to minimize edge effects. The systems were neutralized with counter-ions. The solvated systems were first optimized by conjugate gradient energy minimization combined with a steepest descent minimization performed every 100 steps. Subsequently, the systems were subjected to restrained MD simulations for 100 ps at 300 K, where the protein atoms were harmonically restrained to their initial position with a force constant of 1000 kJ mol^{-1} nm^{-2} to allow the solvent to equilibrate. The optimization phase was followed by unrestrained MD simulations at 300 K. The simulations were carried out in the NVT ensemble using the velocity rescaling thermostat [31] with separate protein and solvent coupling at the reference temperature of 300 K. The v-rescaling method has been shown to give a better distribution of the kinetic energy over the commonly used Berendsen thermostat [31]. The long-range electrostatic interactions were evaluated using the particle mesh Ewald method [32] with a grid size of less than 0.12 nm. A time step for integration of the potential function of 2 fs and non-bonded cutoffs of at least 9 Å were used for all MD simulations. The SHAKE algorithm [33] was used for all covalent bonds. All the MD simulations in explicit water were carried out using an improved version of the AMBER99-SB force field, AMBER99SB-ILDN [34] as implemented in GROMACS 4.5.3.

2.2.3. Analysis of the MD trajectories

Analysis of the MD trajectories was mainly focused on monitoring the secondary structure during the MD simulations using the DSSP criteria [35] through the *do_dssp* module of GROMACS. Cluster analysis used the *g_cluster* module of GROMACS. Root-mean-square-deviation (rmsd) calculations were carried out using the *rmsd trajectory* tool of the VMD software [36]. Principal component analysis was done using the *g_covar* module of GROMACS and the root-mean-square fluctuation of the C^{α} atoms (rmsf C^{α}), which is equal to the square root of the sum of the eigenvalues divided by the number of C^{α} atoms used in building the fluctuation covariance matrix, was employed as an additional metric of the backbone dynamics during a simulation. The VMD program was also employed for visualization of the trajectories, whereas molecular model illustrations were rendered using PyMOL.

2.3. Expression of recombinant proteins and binding assays

SRPK1, the N-terminal domain of chicken LBR (LBRNt, amino acids 1–205) and LBRNt missing the RS motifs (deletion of residues 75–84; construct termed LBRNtΔRS) were subcloned into the pGEX-2T bacterial expression vector (Amersham Pharmacia Biotech) and expressed in bacteria as GST fusion proteins as previously described [19,20]. To eliminate the associated RNA molecules, bacterial preparations of GST-LBRNt (2–3 μg of the recombinant protein) were treated with 5 μg RNAse (Applichem GmbH, DNAse free) for 15 min at 30 °C.

Incubation of GST, GST-LBRNt and GST-LBRNtΔRS immobilized on glutathione-Sepharose beads with 293 T cell extracts (~200 μg of total protein; 293T cells express large amounts of SRPK1) was performed in PBST (20 mM phosphate buffer, pH 7.4, 150 mM NaCl, 1% Triton X-100, and 0.5 mM phenylmethylsulfonyl fluoride) in a total volume of 0.25 ml for 60 min at room temperature. Bound SRPK1 was analyzed on 10% SDS-polyacrylamide gels and detected by Western blotting using an anti-SRPK1 monoclonal antibody (BD Biosciences CA USA) and an alkaline phosphatase-coupled goat antimouse secondary antibody, while 5-bromo-4-chloro-3-indolyl phosphate and nitro blue tetrazolium were used as substrates to visualize the immunocomplexes.

Kinase assays were carried out in a total volume of 25 μl containing 12 mM Hepes pH 7.5, 10 mM $MgCl_2$, 0.5 mM ATP, 2 μg of GST-LBRNt and 0.2 μg GST-SRPK1, for 60 min at 30 °C. The concentration of cold ATP added in the reaction mixture was at the millimolar range to achieve a stoichiometric phosphorylation.

Incubation of GST and GST-LBRNt (either unphosphorylated or phosphorylated) immobilized on glutathione-Sepharose beads with 2 μg of histone H3 (Roche Applied Science) was performed in TNMT buffer (20 mM Tris–HCl, pH 7.5, 0.5 M NaCl, 2 mM $MgCl_2$, and 1% Triton X-100) in a total volume of 0.25 ml. The incubations were carried out for 60 min at room temperature. The beads were harvested, washed three times with TNMT, and resuspended in 25 μl of SDS sample buffer. Bound H3 was analyzed on 13% SDS-polyacrylamide gels and detected by Coomassie Blue staining.

3. Results and discussion

3.1. The unphosphorylated RS repeats adopt flexible conformations composed of short, transient helical elements involving two consecutive RS dipeptides at the time

Sequence analyses have predicted the RS domains to be largely unstructured mainly due to the low sequence complexity of the RS repeats [10,37]. By contrast, an α-helical, instead of the expected random-coil conformation, was observed using all-atom molecular dynamics (MD) simulations on the eight consecutive RS dipeptides, $(RS)_8$, of the RS domain of the splicing factor ASF/SF2 [15]. Subsequent circular dichroism (CD) experiments, however, did not show any significant helical content for the full RS domain of ASF/SF2 [13] suggesting that the helical structure is either too short or may be largely unstable in solution. Adding to the latter, the crystal structure of the SR protein kinase 1 (SRPK1) complexed to its substrate ASF/SF2, revealed that the three N-terminal RS repeats of ASF/SF2 bind to SRPK1 in a rather extended conformation before the phosphorylation reaction [13].

Based on these observations we sought to investigate the conformation of the significantly shorter RS domain of human and turkey lamin b receptor, LBR, consisting of four and five RS dipeptides, respectively. To this end, the $(RS)_4$ and $(RS)_5$ peptides, in a starting completely unfolded state, were first subjected to 200 ns molecular dynamics simulations at 300 K with implicit Generalized Born solvation using various Amber force fields. First, the all-atom AMBER03 force field [27] combined with the Still implicit solvent model [26] was employed, for comparison with the similar work on the $(RS)_8$ peptide [15]. As shown in Fig. 1A, our simulations resulted in a predominantly α-helical conformation undergoing, however helix-to-turn transitions in several segments for both the $(RS)_4$ and $(RS)_5$ peptides. An exclusively α-helical structure was also acquired by the shorter, $(RS)_4$ peptide, using the AMBER96 force field combined with the OBC(II) implicit solvent model (Fig. 1B). This combination was tested as it has been shown to provide reliable structure predictions for various peptides [28]. Our MD results were so far in line with the MD simulation data obtained in the case of the $(RS)_8$ peptide [15], which, however, contradicted the CD data of the RS domain of ASF/SF2 [13].

To rule out the possibility of force field bias for α-helix, the implicit simulations were repeated using the AMBER99SB force field, which has been shown to provide better balance of secondary structure elements [21]. As shown in Fig. 1C, these simulations resulted in more flexible structures with various short segments, extending to only two repetitive RS repeats, adopting short transient α- or 3_{10}-helix-like conformations.

To further investigate the stability of the initially predicted α-helical conformation, an additional 50 ns long MD simulation was carried out, but in explicit solvation, which is a more realistic environment. For this purpose, the resulting helical structure from one of the MD simulations of the $(RS)_5$ peptide was, first, solvated in a periodic cubic box with an edge of approximately 3.5 nm filled with 1658 TIP3P water molecules and neutralized with five chloride ions. The

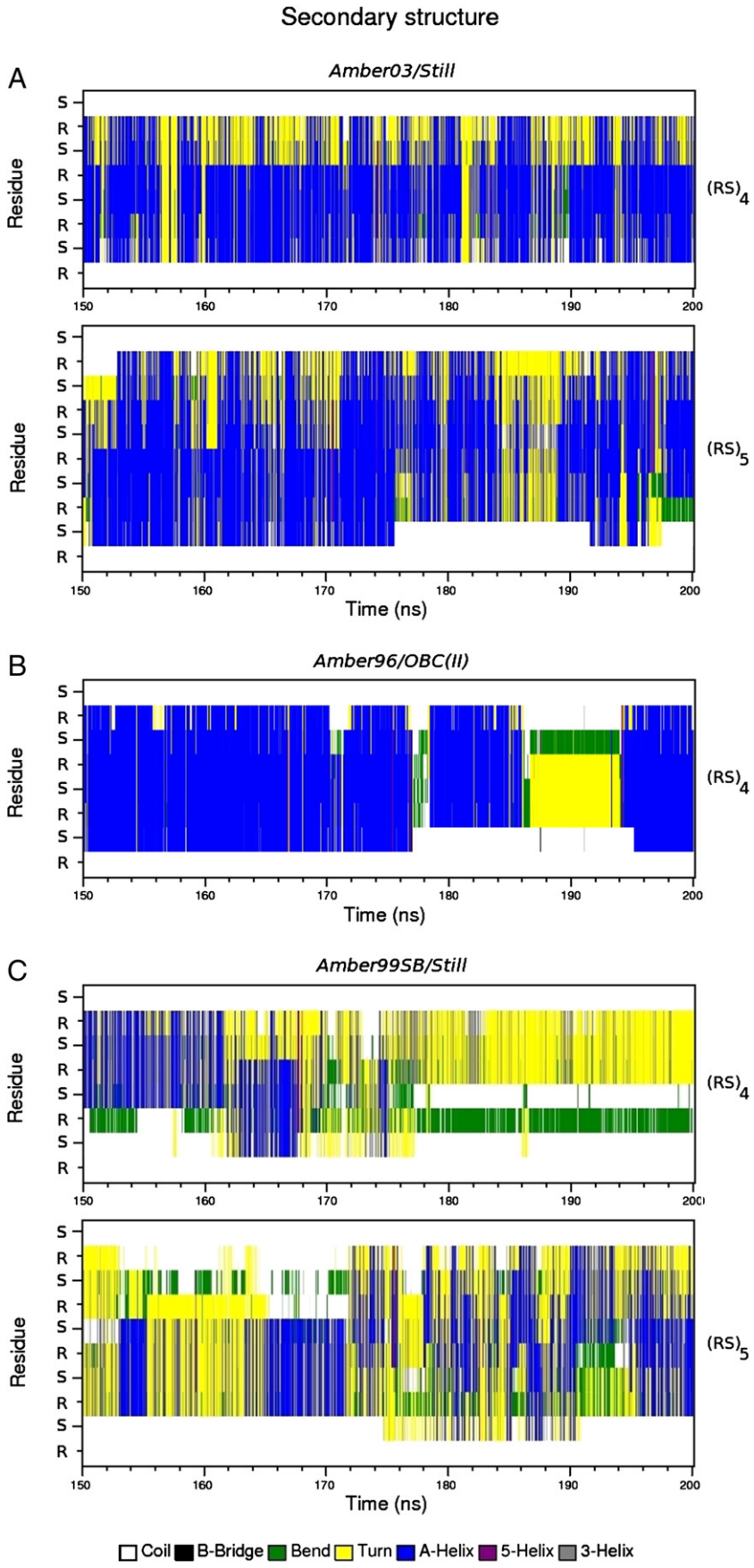

Fig. 1. DSSP analysis of the implicit MD simulations of the unphosphorylated $(RS)_4$ and $(RS)_5$ peptides. Monitoring of the secondary structure along the last 50 ns of the 200 ns MD trajectories resulting by using A) the AMBER03 force field combined with the Still solvation model, B) the AMBER96 force field combined with the OBC(II) solvation model and C) the AMBER99SB force field. The colouring of the secondary structure elements is as indicated in the bottom of the figure.

solvation box was large enough to allow any necessary rotation or potential unfolding of the initial α-helix. As shown in Fig. 2A, the overall α-helix does not persist throughout the explicit MD simulation. Instead, within 50 ns the initial helical structure changed to a more flexible conformation resulting from the formation of transient short α- or 3_{10}-like features (Fig. 2A), in line with our AMBER99SB MD results in implicit solvation. As indicated by the percentage of simulation time each residue spent in the helical (α- or 3_{10}) conformation over the entire simulation (Fig. 2B), the somewhat higher helical propensity is restricted mainly to the central RS dipeptides. The 50 ns trajectory was subsequently clustered and the most populated conformation is shown in Fig. 2C (*right*). In this conformation, the peptide forms one α-turn comprising only two, out of the five, RS dipeptides (Fig. 2C). Such turn-like conformations, allow the arginine residues of the involved RSs, to protrude outward from the peptide backbone.

Our MD results using the AMBER99SB force field are in good agreement with the CD data on the RS domain of ASF/SF2 [13]. Taken together these data suggest that consecutive unphosphorylated RS repeats, although they do not adopt helical structures throughout their length, are able to form transient short helical structural elements involving only two RS repeats at the time, exposing arginine residues of the repeats involved to the solvent, probably thus serving as molecular recognition sites in the interactions of RS-repeat containing proteins. Structurally dynamic regions with temporal presence of secondary structure have been indeed proposed to play an important role in molecular recognition [[38] and references therein]. Due to the highly symmetric character of the RS repeats, however, the exact sequence location of the helical structural elements along the peptide chain is probably not important and the recognition may be based on ensembles of similar conformations. In line with this idea, the number of the RS repeats varies significantly not only among LBRs but also among RS-containing proteins, in general.

3.2. Identification of a docking motif in LBR

The RS-rich region of LBR is recognized and gets phosphorylated on serine residues by multiple RS kinases in a cell cycle-dependent manner [19,39,40]. One such kinase is SRPK1, which was originally described as a kinase highly specific for the SR splicing factors [41]. SRPK1 has been shown to be able to phosphorylate any one of the serine residues of the RS repeats of turkey LBR as long as those RS dipeptides are followed by the downstream flanking sequence, PGRPAKG [19,20].

Multiple alignment of LBR sequences revealed that the region involving the flanking sequence as well as the three C-terminal RS dipeptides, is conserved among LBR sequences (Fig. 3A). Interestingly, this conserved sequence conforms to the consensus seven aminoacid motif, R-x-R/K-x-x-x-R, known as the docking motif sequence [12]. This motif has been proposed to constitute a recognition platform for SRPK1 and has been shown to bind to an acidic groove, distal from the active site, known as the "docking groove", through nearly perfect charge complementarity involving the two basic residues at motif positions 1 and 7, while the side chain of the arginine at position 3 is buried in a deep hydrophobic pocket of the groove [12,13].

To test the possibility that this region of LBR also serves as a docking motif for SRPK1, a 3D-model of the ^{78}SRSRSRSPGR^{87} peptide of LBR (peptide R2′) bound to SRPK1 was first constructed (Fig. 3B), based on the crystal structure of a 10-mer substrate peptide from ASF/SF2 protein in complex with SRPK1 (RCSB code: 3BEG) [13]. In the 3D-model of the SRPK1:LBR R2′ peptide complex, the docking interactions of the template structure are preserved: the two basic residues of LBR at motif positions 1 and 7 (Arg 81 and Arg 87, respectively) form electrostatic interactions with the same acidic residues of the SRPK1 docking groove (Asp 564, Glu 571 and Asp 548) [12], whereas the arginine residue at position 3 (Arg 83) is buried in the same hydrophobic pocket (Fig. 3B). The initial model was subsequently subjected to a set of MD simulations, in explicit water, using the peptide both in isolation and in complex to SRPK1, to gain insight into its conformation in the absence and presence of the kinase, respectively.

For this purpose, first the peptide alone (Fig. 3C, *left*) was solvated in a periodic cubic box with an edge of 3.3 nm filled with 1129 TIP3P water molecules and neutralized with four chloride ions. The explicit simulation was performed for 30 ns, as described in Materials and methods. The DSSP analysis [35] of the 30 ns trajectory revealed again some preference for helical conformations for the central two RS repeats, whereas the C-terminal RS together with its flanking

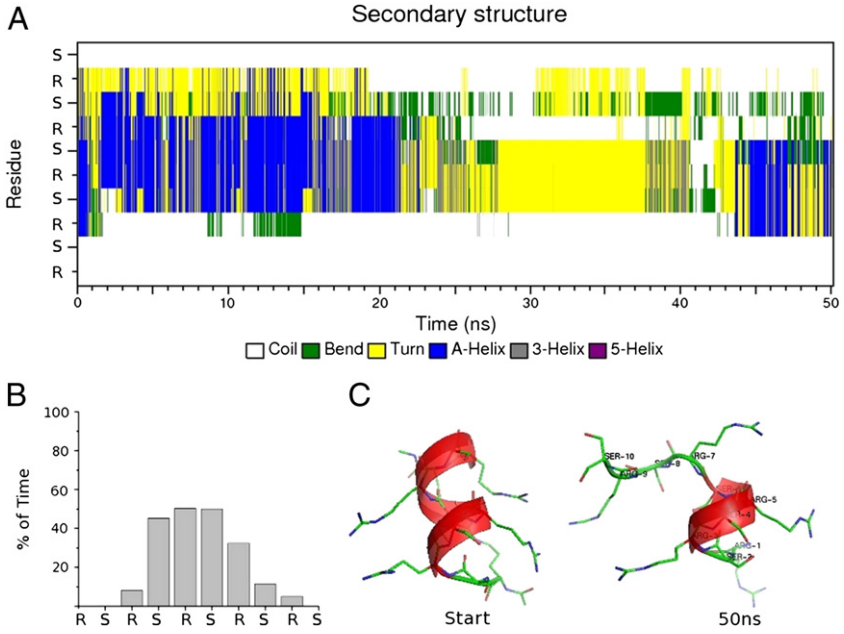

Fig. 2. Analysis of the explicit MD simulation of the helical unphosphorylated $(RS)_5$ peptide. A) DSSP analysis of the 50 ns explicit MD trajectory B) Percentage of simulation time each residue spends in helical (α- and 3_{10}-) conformations throughout the entire simulation. C) The starting α-helical (*Left*) and the resulting (*Right*) conformation after the 50 ns simulation (the most populated cluster within the last 10 ns). The program PYMOL was used for preparing panel C.

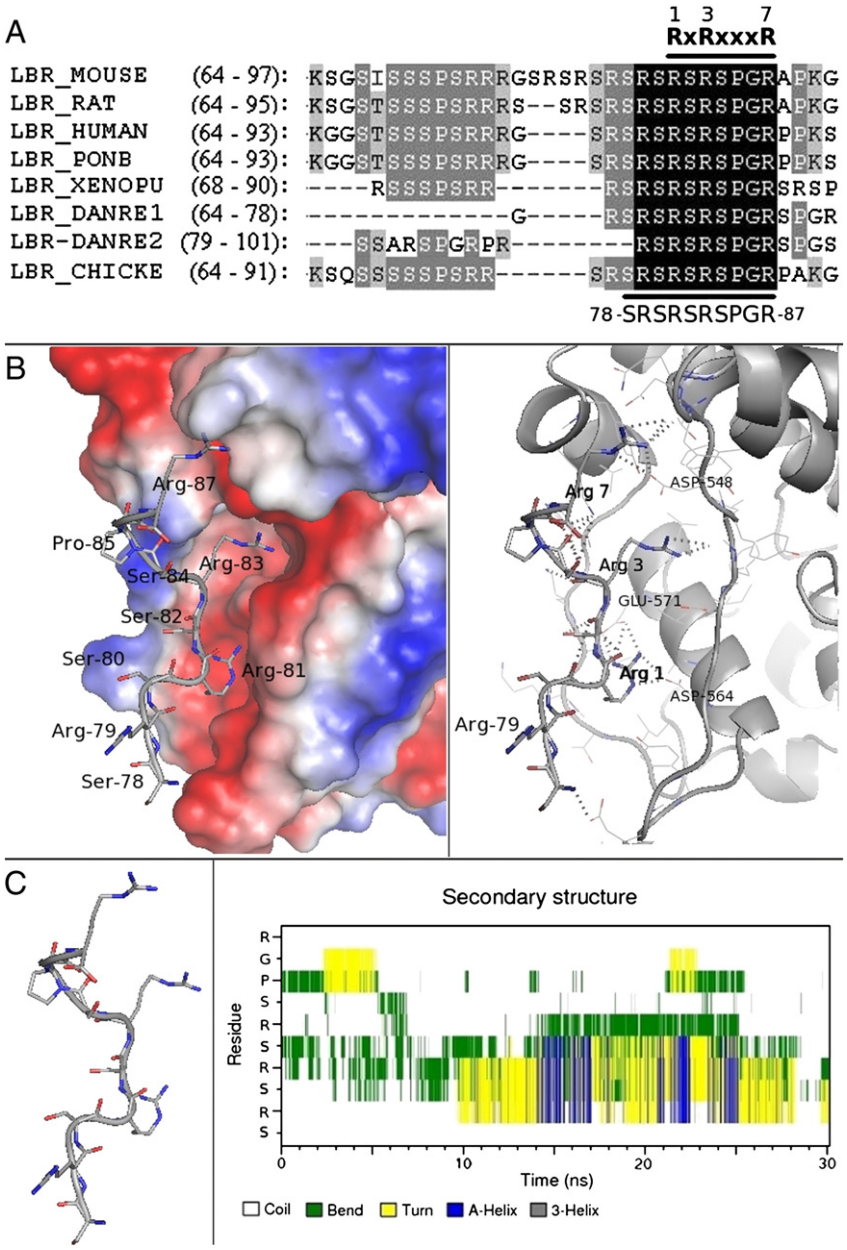

Fig. 3. The LBR "docking peptide", R2′. A) Multiple alignment of LBR sequences edited using GeneDoc [22]. The conserved sequence is black shaded. The consensus sequence corresponding to the docking motif is indicated above the alignment. The region of aa: 78–87, corresponding to the R2′ peptide (docking peptide) used for the MD simulations in regard to SRPK1 kinase, is also indicated. B) The 3D-model of the R2′ peptide (in sticks) docked to the docking domain of SRPK1 (surface coloured by the electrostatic potential (*Left*) and in ribbon representation (*Right*)). The program PYMOL was used for preparing these illustrations. Dotted lines indicate H-bonding interactions. Important residues are labelled. C) Analysis of the 30 ns MD simulation of the free LBR R2′ peptide in explicit water (*Left*) The starting conformation of the free peptide used in the 30 ns MD simulation and (*Right*) DSSP analysis of the 30 ns trajectory. The N-terminal RS region has some propensity for helical conformations, while the C-terminal region of the peptide remains rather unstructured during the entire simulation.

region retained a rather extended conformation (Fig. 3C, *right*). These results, in conjunction with our MD data on the RS peptides, suggest that, in their unbound form, the consecutive LBR RS repeats have some propensity for helical conformations of one turn, whereas terminal RSs and their flanking regions remain rather unstructured, probably thus contributing further to recognition and binding to SRPK1.

To investigate the stability of R2′ peptide structure in the presence of SRPK1, an additional 20 ns long explicit MD simulation was carried out. For this purpose, the 3D-model of the SRPK1:R2′ peptide complex we constructed, was first solvated in a $6.2 \times 6.8 \times 7.1$ nm periodic box filled with 8794 TIP3P water molecules and neutralized with four chloride ions. This MD simulation was performed using the improved AMBER99SB, AMBER99SB-ILDN, force field [34], as described in Materials and methods. The root-mean-square fluctuation (rmsf) of the C^{α} atoms within the last 5 ns of the trajectory was equal to 0.68 Å and the root-mean-square deviation (rmsd C^{α}) from their initial positions remained practically unchanged for the same time period (the standard deviation was equal to 0.11 Å for the protein and 0.23 Å for the peptide) (see also Supplementary Fig. S1), indicating that the simulation is converged and that the resulting structure of the SRPK1:R2′ complex is quite stable. As shown in Fig. 4A, the initial docking interactions between LBR basic residues at motif positions 1, 3 and 7 and the docking groove of SRPK1 persist after 20 ns (compare Figs. 3B, *right* and 4A, *right*). More precisely, during the entire 20 ns MD simulation, the arginine residues at positions 1 and 3 experience small fluctuations, as reflected by the relatively small rmsd of all their atoms from their initial positions (Fig. 4B, *left*; in blue and green,

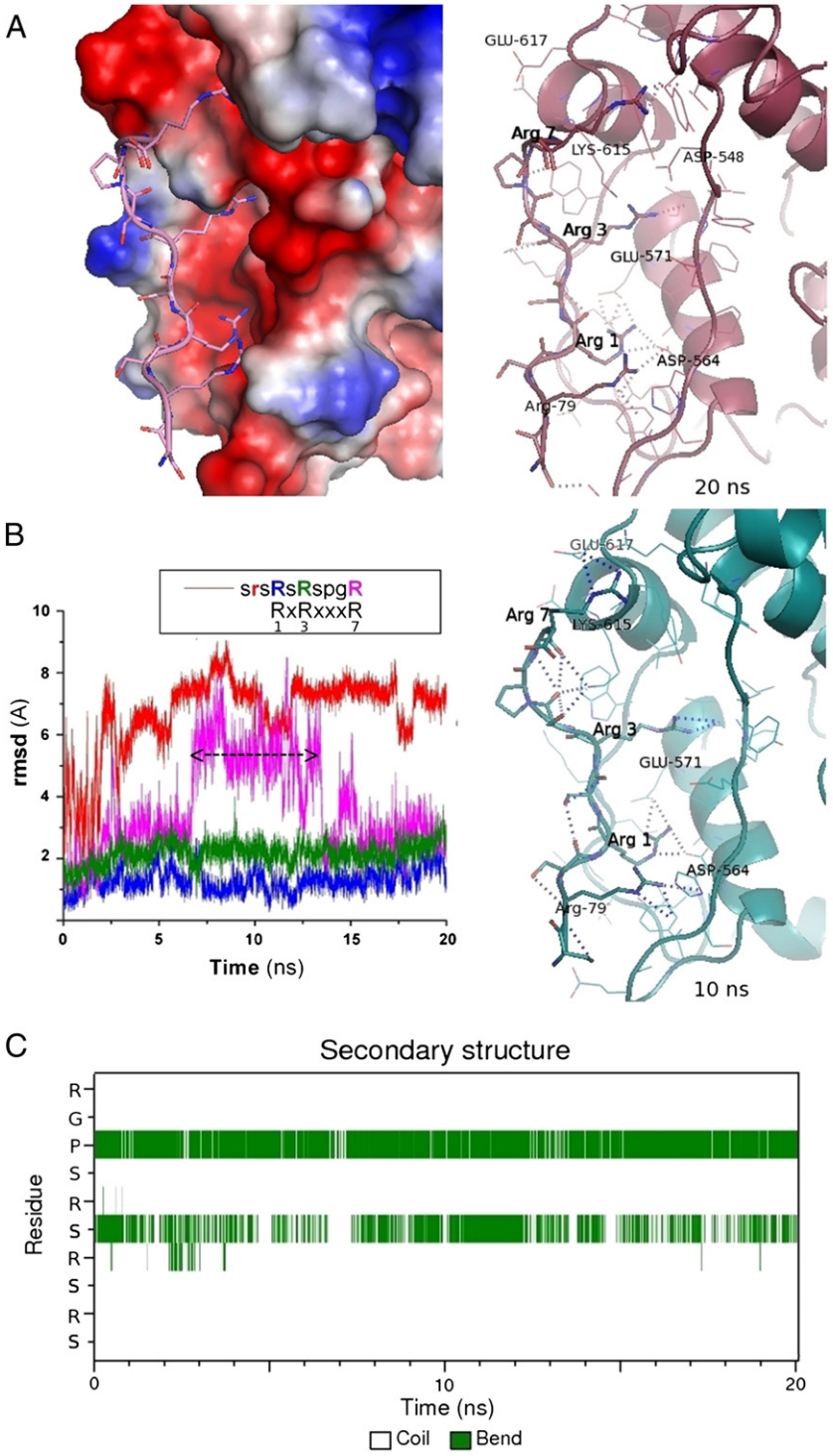

Fig. 4. Analysis of the 20 ns explicit MD simulation of the SRPK1:LBR R2′ peptide complex. A) The resulting conformation after the 20 ns explicit MD simulation of the LBR R2′ peptide (in sticks) complexed to SRPK1. The picture is depicted as in Fig. 3B. The docking interactions between the arginine residues of the R2′ peptide and acidic residues of the SRPK1 groove (D564, E571, D548) remain unchanged (compare with Fig. 3B, *right*). Arginine 79 of the upstream the docking motif region is now H-bonded to D564 of SRPK1. B) (*Left*): Plot of the root-mean-square deviation (rmsd) of all the atoms of the basic residues of the R2′ peptide from their initial positions during the 20 ns trajectory. Blue, green, magenta and red lines correspond to rmsds of arginine residues at motif positions 1, 3 and 7 and of the upstream region, respectively. The arrow indicates a cluster of an alternative conformation of Arginine at motif position 7. (*Right*) The 10 ns snapshot. The arginine at position 7 is hydrogen bonded to E617 instead of D548 (see Fig. 3A, *right*). C) Secondary structure analysis (DSSP) of the 20 ns trajectory for the R2′ peptide. The RS region of the peptide remains unfolded during the entire MD simulation in the presence of SRPK1.

respectively), indicating that the docking interactions they are involved in, are very stable. In particular, the side chain of the arginine at position 1 (Arg 81) remained hydrogen bonded to Asp 564 and Glu 571 of the SRPK1 docking groove for 99% of the simulation time (data not shown), suggesting an important role of these residues of SRPK1 in LBR recognition. By contrast, arginine at position 7 (Arg 87) was more mobile (Fig. 4B, *left*; in magenta) sharing its time between conformations where its side chain interacted with either Asp 548 (Fig. 4A, *right*) or Glu 517 (at around 10 ns; Fig. 4B, *right*). The acidic residues D548, D564 and E571 have been shown to be important for

recognition of ASF/SF2 by SRPK1 [12], whereas homologous residues have been shown to be important for substrate recognition by the SRPK1 homologue, Sky1p [14]. Taken together these observations strongly suggest that the same acidic residues of the docking groove of SRPK1 as well as Glu 517 may also be important for the recognition of LBR by SRPK1.

By contrast to the docking motif basic residues, Arg 79, which belongs to the adjacent the docking motif, RS region (Fig. 1A) undergoes a large movement, as indicated by the large rmsd value of all its atoms from their initial position along the 20 ns trajectory (Fig. 4B, *left*; in red). Within 10 ns, this residue flipped its side chain towards SRPK1, forming hydrogen bonding interactions with Asp 564 (Fig. 4B, *right*). Once formed, these interactions remain stable during the rest of the simulation (compare Fig. 4A and B, *right*). Interestingly, as indicated by the secondary structure analysis (DSSP plot) of the 20 ns trajectory, the whole RS region of the R2′ peptide remains unfolded during the entire simulation in the presence of SRPK1 (Fig. 4C), by contrast to the helical conformation suggested by our MD simulations for this region in the free peptide (Fig. 3C, *right*). Our observations so far, suggest that binding to SRPK1 may promote a complete unfolding of the RS repeats of LBR.

To further investigate whether the sequence of the RS domain of LBR possesses the potential to adopt alternative conformations as influenced by changes in tertiary environment, a contact-dependent secondary structure prediction was carried out using the neural network-based predictor, CSSP2 [42] and the RS domain sequence of turkey LBR, as query. The CSSP2 tool quantifies the influence of tertiary effects on secondary structure preferences by using energy-based parameters, which take into account either short-range (i, i ± 4) or long-range (>i, i ± 4) interactions [[42] and references therein]. The CSSP2 (dual networks) secondary structure profiles of the RS domain of LBR are shown in Fig. 5A. When short-range interactions (i, i ± 4) are taken into account, a relatively higher helix propensity is predicted for the RS repeats of LBR, as compared to non-RS regions (Fig. 5A, *red line*), suggesting some inherent preference of consecutive RS dipeptides for α-helical conformations. By contrast, the conformational preference of the RS repeats changed in favor of a more extended (beta-like) structure (Fig. 5A, *blue line*) when long-range interactions (>i, i ± 4) are taken into account, instead. For comparison, the CSSP2 program was used to predict the secondary structure of the RS domain of ASF/SF2. As shown in Fig. 5B, the CSSP profiles also suggest a similar propensity for α-helix for the RS repeats of ASF/SF2 and a potential to undergo similar conformational changes in different tertiary environments, in agreement with the extended conformation revealed by the crystal structure of the 10-mer peptide of ASF/SF2 (underlined sequence in Fig. 5B) bound to SRPK1 [13]. Interestingly, the region corresponding to the proposed docking motif of LBR (indicated by a bar above the sequence in Fig. 5A) did not show any significant preference for α-helix formation, but its larger part is predicted to be rather unstructured in all environments (Fig. 5A), further supporting its proposed role as a molecular recognition site. These results, in conjunction with our MD simulation data on the R2′ peptide in both its free and bound to SRPK1 forms, suggest that consecutive RS dipeptides have some inherent propensity for α-helix formation, whereas binding of LBR to SRPK1 through its docking motif, may induce an unfolding of adjacent RS dipeptides, mediated by electrostatic interactions involving the arginine residues of the RS dipeptides and acidic residues of the SRPK1 docking groove. The unfolding of the RS repeats destined to be phosphorylated might be necessary for their subsequent phosphorylation by SRPK1. Unfolding of their substrates has been also proposed in the case of other kinases, including SRPK1 [[13] and reference therein]. In support to this idea, a construct containing only the five RS dipeptides of LBR but lacking the docking motif, although it could serve as substrate for SRPK1, it was phosphorylated at a minimal extent as compared to native LBR [20].

Taken together, our results suggest that the ^{81}RSRSPGR^{87} peptide of LBR (turkey nomenclature), extending downstream the RS repeats, may serve as a docking region to SRPK1, being thus necessary for phosphorylation of its RS repeats. In line with this idea, an RS-containing peptide of turkey LBR (R1: KQRKSQSSSSSPSRRSRSRS) lacking the proposed docking motif, could not be phosphorylated by SRPK1, while a significantly shorter peptide (R2: SRSRSRSPGRPAK) comprising this region, was phosphorylated to a similar extend as wt-LBR [20].

Interestingly, the docking motif we propose in this study overlaps with the RS dipeptides of LBR, suggesting that the RS repeats are also necessary for the recognition of LBR by SRPK1. Previous data support this suggestion as binding experiments of the purified LBR kinase from turkey erythrocytes to LBR showed that the kinase was able to associate with GST-LBRNt (aa: 1–205), whereas no binding was observed when a similar construct lacking the five RS dipeptides (GST-LBRNtΔRS) was used instead [19]. Even though in subsequent studies, LBR kinase was shown to be SRPK1 [20,43–45], we repeated the binding experiments using an anti-SRPK1 specific monoclonal antibody, to further test the ability of SRPK1 to bind LBR in the absence of its RS repeats. As shown in Fig. 6, SRPK1 binds to LBRNt with significant affinity but fails to associate with LBRNtΔRS, indicating that the RS repeats are important for the binding of LBR by SRPK1. Interestingly, part of the RS1 region of ASF/SF2 destined to be phosphorylated has also been shown to serve as a docking site for SRPK1 before initiation of the phosphorylation reaction [13], implying that the RS repeats of ASF/SF2 are also part of its docking motif. Taken together these observations suggest for the first time that the RS repeats apart from phosphorylation sites may constitute integral part of docking motifs for SRPK1.

Our data so far, in conjunction with prior knowledge allow as to propose that the RSRSPGR peptide of LBR constitutes a docking motif for SRPK1 and that the kinase uses the same, distal to the active site, acidic docking groove to recognize it, as its other substrates. Binding of this motif may subsequently induce an unfolding of the RS repeats destined to be phosphorylated. However, due to the short length of the RS domain and its overlapping with the docking site, SRPK1 must use for LBR a different substrate feeding mechanism than the one proposed for the phosphorylation of ASF/SF2 [[11] and references therein].

3.3. Phosphorylation of serine residues of the RS repeats induces the formation of Arg-claw-like structures

Using all-atom MD simulations, it has been previously shown that upon serine phosphorylation, the stretch of eight RS repeats ($(RS^p)_8$), corresponding to the RS1 domain of ASF/SF2, is able to adopt compact, Arg-claw-like conformations proposed to be involved in the recognition, binding and transport of the ASF/SF2 protein [15]. This structure was formed by the guanidinium groups of some of the eight arginine residues, which surround the phosphate moiety of one of the phosphoserines.

To investigate whether the significantly shorter RS domain of LBR exhibits similar conformations upon phosphorylation by SRPK1, we carried out an additional implicit molecular dynamics simulation with all four serine residues of $(RS)_4$ phosphorylated (hereafter referred to as $(RS^p)_4$). The four RS dipeptides corresponding to the RS domain of human LBR were preferred over the five RS dipeptides of the chicken orthologue, to rule out the effect of the RS-repeat length in Arg-claw formation. Again a 200 ns simulation with implicit GB solvation was undertaken. Because our data so far suggest an unfolding of the RS dipeptides prior to their phosphorylation, we used a fully extended conformation of the peptide, as the initial structure. As indicated by the secondary structure analysis of the 200 ns trajectory, unlike the unphosphorylated peptide, the phopsphopeptide does not show any propensity for helical conformations (Fig. 7A, *upper panel*). Instead,

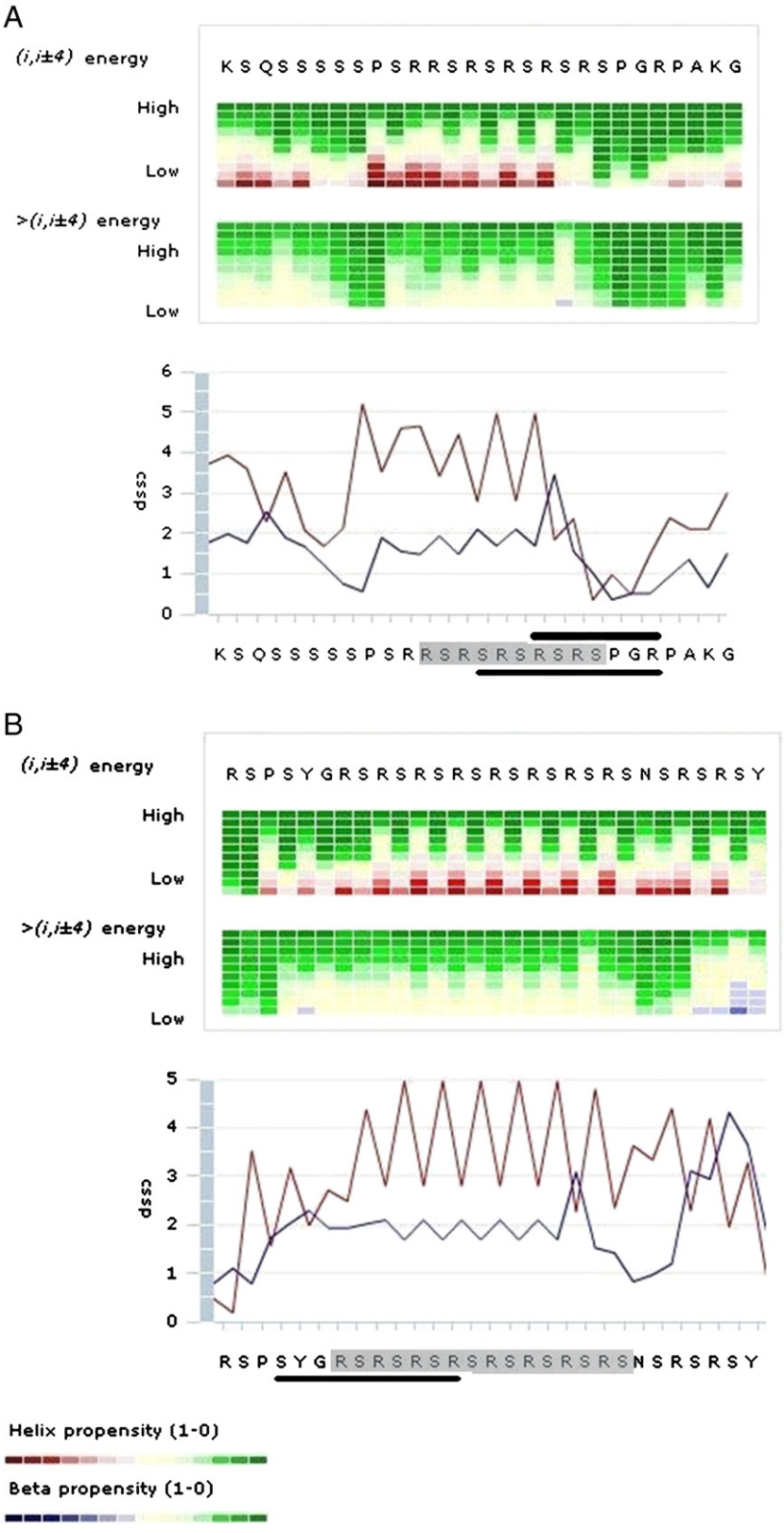

Fig. 5. Contact-dependent secondary structure propensities. CSSP2 (dual networks) profiles [42] of the RS domain of the (A) turkey LBR and (B) human ASF/SF2 proteins. The (i, i ± 4) and > (i, i ± 4) denote profiles based on short- and long-range interactions, respectively. Red, blue and green colors are used for α-helix, extended (β-strand) and random coil, respectively. Consecutive RS dipeptides are grey shaded. The sequences corresponding to the LBR R2′ peptide, used in this study, and to a 10-mer substrate peptide of ASF/SF2, the structure of which bound to SRPK1 has been determined by X-ray crystallography [13], are underlined. Secondary structure propensities are colored as indicated in the bottom of the figure. The profiles show some inherent propensity for α-helix for consecutive RS dipeptides with a potential to undergo conformational changes in different environments, whereas an unstructured conformation is predicted for the proposed docking motif region of LBR (indicated by a black bar above the sequence) in all environments.

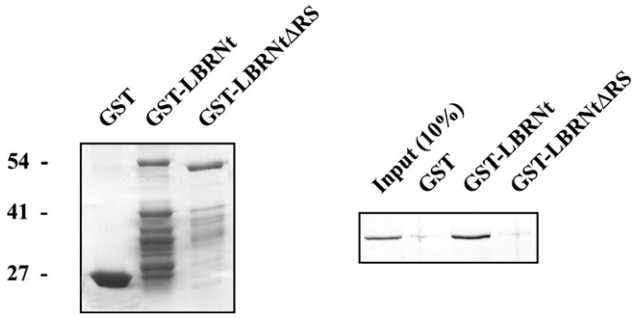

Fig. 6. Association of SRPK1 with LBR. SDS-PAGE analysis and Coomassie Blue staining of GST, GST-LBRNt and GST-LBRNtΔRS (*left panel*). GST pull-down assays show that SRPK1 binds to LBRNt but fails to bind to LBRNtΔRS that lacks the five RS dipeptides (*right panel*).

the conformation of the most populated cluster within the last 50 ns (Fig. 7B , *left*) revealed the formation of an Arg-claw structure, similar to the one found in the case of the significantly longer $(RS^P)_8$ peptide [15]: The guanidinium groups of all four arginine residues are hydrogen bonded to the phosphate group of one phosphoserine (S2P 8).

To test the accuracy of the implicit MD simulation, the Arg-claw conformation was used as the initial structure for an additional 50 ns long MD simulation, but in explicit water. A periodic cubic box filled with 512 TIP3P water molecules was used, for this purpose. The backbone conformation of the peptide remained practically unchanged along the 50 ns trajectory, as shown by the secondary structure analysis (Fig. 7A, *lower panel*) and by the small rmsd of the backbone atoms from their initial positions (mean rmsd equals to 0.6 Å) (Supplementary Fig. S2). Although the number of guanidinium groups around S2P 8 was reduced by one compared to the starting conformation, the compact clawed structure persisted after the 50 ns simulation (Fig. 7B, *right*) indicating that the Arg-claw structure is very stable. This configuration, allows the phosphate groups of the remaining three phosphoserines to protrude outward from the peptide backbone, pointing into solution (Fig. 7B), probably thus serving as recognition sites, as proposed for the ASF/SF2 protein [15].

Our MD simulation data on the phosphorylated $(RS^P)_4$ peptide adding to similar results obtained for the significantly longer $(RS^P)_8$ peptide [15] suggest that the propensity to form Arg-claw structures may be a general property of phosphorylated RS repeats, irrespective of the number of consecutive RS dipeptides.

The phosphorylation-induced formation of Arg-claw configurations and the exposure of the phosphate groups of the phosphoserines to the periphery may widen the association repertoire of LBR, including also partners rich in basic residues.

3.4. Phosphorylation of the RS domain of LBR protein regulates its association with histone H3

In a previous work we demonstrated that the core histones H3 and H4 could associate with the N-terminal domain of LBR and that this

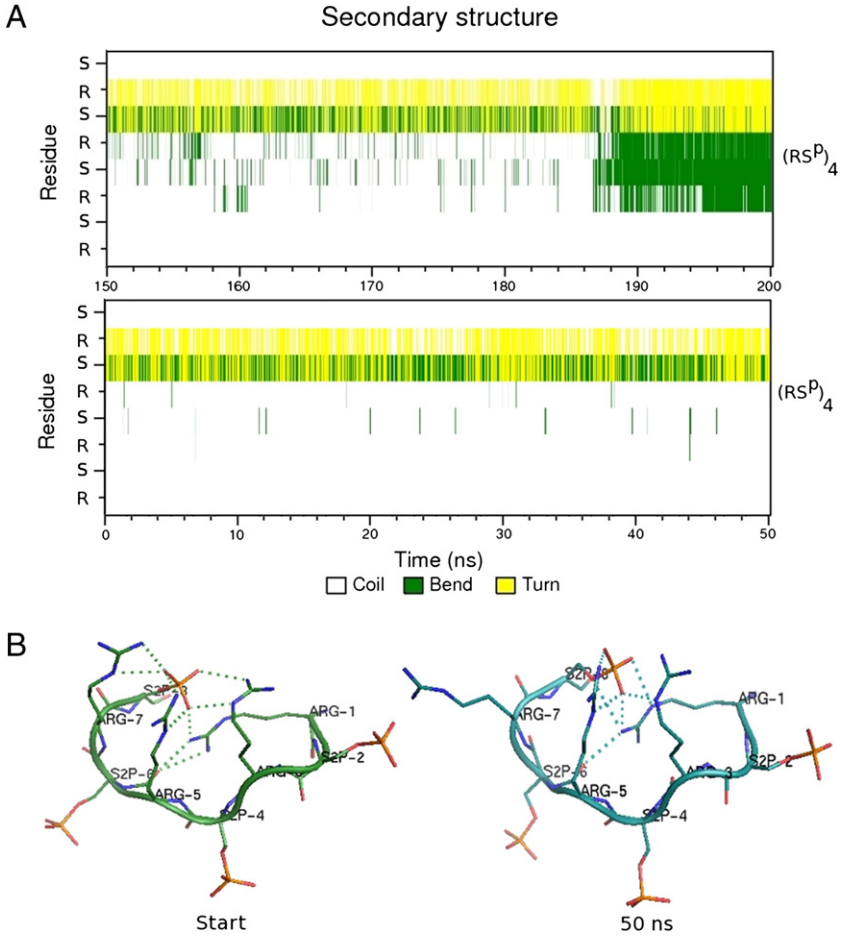

Fig. 7. Analysis of the MD simulations of the fully phosphorylated peptide, $(RS^P)_4$. A) DSSP analysis of the last 50 ns of the 200 ns MD trajectory with implicit solvent (*Upper panel*) and of the 50 ns MD trajectory, in explicit water (*Lower panel*) B) (*Left*) The conformation of the most populated cluster within the last 50 ns of the implicit MD simulation used as initial structure for the explicit MD simulation in explicit water (*Right*) The final conformation after the 50 ns MD simulation, in explicit water. Hydrogen bonds are shown by dashed lines. The formed Arg-claw persists after the 50 ns MD simulation, suggesting the ability of the phosphorylated $(RS^P)_4$ peptide to also form Arg-claws as shown in the case of the significantly longer peptide, $(RS^P)_8$ [15].

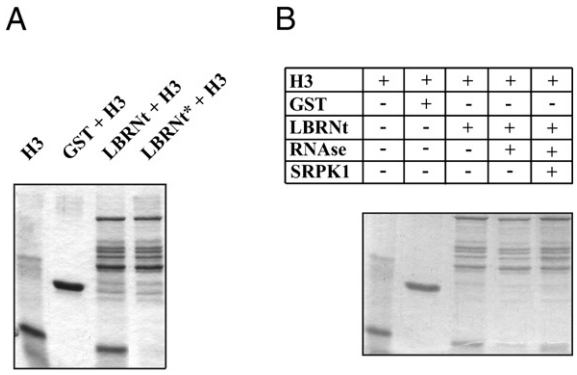

Fig. 8. Interaction of LBR with histone H3. A) Pull-down assays show that H3 binds to bacterially produced GST-LBRNt but fails to bind to GST-LBRNt treated with RNAse prior to the binding assay (denoted by an *asterisk*). B) Phosphorylation of GST-LBRNt (pretreated with RNAse) restores the binding of H3 (*lane 5*). GST, GST-LBRNt and GST-LBRNt treated only with RNAse were included as controls (*lanes 2, 3* and *4*, respectively). Bound H3 was detected by Coomassie Blue staining.

association was not affected when nuclear envelope extracts or the purified recombinant protein (GST-LBRNt) were pre-digested with DNAse I, indicating that DNA was not involved in these interactions [46]. At first site this binding is "out of the ordinary" from a structural point of view, since both histones and LBRNt have a high positive charge (pI > 10). In light of our new data, we investigated the role of phosphorylation of LBRNt in this association. To this end, we first repeated the binding assays but this time using GST-LBRNt depleted of the associated bacterial RNA molecules following RNAse treatment. This experiment was performed in order to rule out the role of RNA in this particular interaction. As shown in Fig. 8, RNA digestion of GST-LBRNt preparations (denoted with an asterisk in Fig. 8A) totally abolished the binding of H3 to the recombinant protein (Fig. 8A and B, *lane 4*). However, subsequent phosphorylation of GST-LBRNt by GST-SRPK1 significantly promoted the association of histone H3 with GST-LBRNt (Fig. 8B, *lane 5*). Our data indicate that the core histone H3 does not bind directly to the unmodified LBR, and the previously observed binding [46] was mediated by bacterial non sequence-specific RNA molecules bound to LBR. The H3/LBR association is possible only upon phosphorylation of the RS repeats of LBR, probably due to the formation of recognition elements induced by Arg-claw-like structures, with the phosphogroups protruding to the solvent and being available for recognition by the basic residues of the H3 tail.

4. Conclusions

In this study, we used a combination of molecular dynamics simulations and biochemical approaches to shed light into the phosphorylation of the RS domain of lamin b receptor by SRPK1.

From the methodology point of view, we found that, among the force fields tested only the Amber99SB force field was able to produce reliable MD results. Our MD simulations revealed that the unphosphorylated RS repeats of LBR follow flexible structures consisting of short, transient helical elements including only two consecutive RS dipeptides at the time. On the other hand, our MD simulations on the phosphorylated $(RS^p)_4$ peptide showed that serine phosphorylation of the RS repeats induces the formation of an Arg-claw-like structure, exposing phosphate groups to the periphery, very much alike the one found in the case of the phosphorylated RS domain of ASF/SF2 [15]. Thus, the tendency to form Arg-claw-like structures, serving as molecular recognition elements that mediate the interactions of RS-repeat containing proteins with basic biological partners such as histone H3, may be a general property of phosphorylated RS repeats, irrespective of their length.

Furthermore, we provide evidence that the highly conserved in all LBRs RSRSPGR peptide, overlapping with the RS repeats, may constitute a docking motif for SRPK1. A role of this docking interaction in the unfolding of the RS repeats destined to be phosphorylated is suggested by our MD simulations. We propose that SRPK1 uses the same, distal to the active site, acidic docking groove to recognize the suggested basic docking motif of LBR, as its other substrates. However, because of the short length of the RS repeats of LBR and their partial overlapping with the proposed docking motif, SRPK1 must use for LBR a different substrate feeding mechanism than the one proposed for the phosphorylation of proteins with long RS domains [11].

Acknowledgements

This work was partly supported by the DEMOEREVNA and the Post-doctoral Fellowships programs of NCSR "Demokritos". Nikolas Voukkalis was a recipient of a fellowship from Onassis Foundation.

Appendix A. Supplementary data

Supplementary data to this article can be found online at doi:10.1016/j.bbagen.2011.10.010.

References

[1] D. Hamelberg, T. Shen, J.A. McCammon, Phosphorylation effects on cis/trans isomerization and the backbone conformation of serine-proline motifs: accelerated molecular dynamics analysis, J. Am. Chem. Soc. 127 (2005) 1969–1974.
[2] L.M. Iakoucheva, P. Radivojac, C.J. Brown, T.R. O'Connor, J.G. Sikes, Z. Obradovic, A.K. Dunker, The importance of intrinsic disorder for protein phosphorylation, Nucleic Acids Res. 32 (2004) 1037–1049.
[3] A. Narayanan, M.P. Jacobson, Computational studies of protein regulation by post-translational phosphorylation, Curr. Opin. Struct. Biol. 19 (2009) 156–163.
[4] H. Li, P.M. Bingham, Arginine/serine-rich domains of the su(wa) and tra RNA processing regulators target proteins to a subnuclear compartment implicated in splicing, Cell 67 (1991) 335–342.
[5] R. Boucher, C.A. Ouzounis, A.J. Enright, B.J. Blencowe, A genome-wide survey of RS domain proteins, RNA 7 (2001) 1693–1701.
[6] T. Giannakouros, E. Nikolakaki, I. Mylonis, E. Georgatsou, Serine–arginine protein kinases: a small protein kinase family with a large cellular presence, FEBS J. 278 (2011) 570–586.
[7] B.R. Graveley, Sorting out the complexity of SR protein functions, RNA 6 (2000) 1197–1211.
[8] H. Shen, M.R. Green, A pathway of sequential arginine–serine-rich domain-splicing signal interactions during mammalian spliceosome assembly, J. Mol. Cell. 16 (2004) 363–373.
[9] H. Shen, M.R. Green, RS domains contact splicing signals and promote splicing by a common mechanism in yeast through humans, Genes Dev. 20 (2006) 1755–1765.
[10] E. Nikolakaki, V. Drosou, I. Sanidas, P. Peidis, T. Papamarcaki, L.M. Iakoucheva, T. Giannakouros, RNA association or phosphorylation of the RS domain prevents aggregation of RS domain-containing proteins, Biochim. Biophys. Acta 1780 (2008) 214–225.
[11] G. Ghosh, J.A. Adams, Phosphorylation mechanism and structure of serine–arginine protein kinases, FEBS J. 278 (2011) 587–597.
[12] J.C. Ngo, S. Chakrabarti, J.H. Ding, A. Velazquez-Dones, B. Nolen, B.E. Aubol, J.A. Adams, X.D. Fu, G. Ghosh, Interplay between SRPK and Clk/Sty kinases in phosphorylation of the splicing factor ASF/SF2 is regulated by a docking motif in ASF/SF2, Mol. Cell 20 (2005) 77–89.
[13] J.C. Ngo, K. Giang, S. Chakrabarti, C.T. Ma, N. Huynh, J.C. Hagopian, P.C. Dorrestein, X.D. Fu, J.A. Adams, G. Ghosh, A sliding docking interaction is essential for sequential and processive phosphorylation of an SR protein by SRPK1, Mol. Cell 29 (2008) 563–576.
[14] R. Lukasiewicz, B. Nolen, J.A. Adams, G. Ghosh, The RGG domain of Npl3p recruits Sky1p through docking interactions, J. Mol. Biol. 367 (2007) 249–261.
[15] D. Hamelberg, T. Shen, J.A. McCammon, A proposed signaling motif for nuclear import in mRNA processing via the formation of arginine claw, Proc. Natl. Acad. Sci. U. S. A. 104 (2007) 14947–14951.
[16] H.J. Worman, C.D. Evans, G. Blobel, The lamin B receptor of the nuclear envelope inner membrane: a polytopic protein with eight potential transmembrane domains, J. Cell Biol. 111 (1990) 1535–1542.
[17] Q. Ye, H.J. Worman, Primary structure analysis and lamin B and DNA binding of human LBR, an integral protein of the nuclear envelope inner membrane, J. Biol. Chem. 269 (1994).
[18] A. Pyrpasopoulou, J. Meier, C. Maison, G. Simos, S.D. Georgatos, The lamin B receptor (LBR) provides essential chromatin docking sites at the nuclear envelope, EMBO J. 15 (1996) 7108–7119.
[19] E. Nikolakaki, G. Simos, S.D. Georgatos, T. Giannakouros, A nuclear envelope-associated kinase phosphorylates arginine–serine motifs and modulates interactions between the lamin B receptor and other nuclear proteins, J. Biol. Chem. 271 (1996) 8365–8372.

[20] S. Papoutsopoulou, E. Nikolakaki, T. Giannakouros, SRPK1 and LBR protein kinases show identical substrate specificities, Biochem. Biophys. Res. Commun. 255 (1999) 602–607.
[21] V. Hornak, R. Abel, A. Okur, B. Strockbine, A. Roitberg, C. Simmerling, Comparison of multiple Amber force fields and development of improved protein backbone parameters, Proteins 65 (2006) 712–725.
[22] K.B. Nicholas, H.B.J. Nicholas, D.W. Deerfield, GeneDoc: analysis and visualization of genetic variation, EMBNEW. NEWS 4 (1997) 14.
[23] N. Guex, M.C. Peitsch, SWISS-MODEL and the Swiss-PdbViewer: an environment for comparative protein modeling, Electrophoresis 18 (1997) 2714–2723.
[24] B. Hess, C. Kutzner, D. van der Spoel, E. Lindahl, GROMACS 4: algorithms for highly efficient, load-balanced, and scalable molecular simulation, J. Chem. Theory Comput. 4 (2008) 435–447.
[25] D. Sellis, D. Vlachakis, M. Vlassi, Gromita: a fully integrated graphical user interface to gromacs 4, Bioinform. Biol. Insights 3 (2009) 99–102.
[26] D. Qiu, P.S. Shenkin, F.P. Hollinger, W.C. Still, The GB/SA continuum model for solvation. A fast analytical method for the calculation of approximate Born raddi, J. Phys. Chem. A 101 (1997) 3005–3014.
[27] Y. Duan, C. Wu, S. Chowdhury, M.C. Lee, G. Xiong, W. Zhang, R. Yang, P. Cieplak, R. Luo, T. Lee, J. Caldwell, J. Wang, P.A. Kollman, Point-charge force field for molecular mechanics simulations of proteins based on condensed-phase quantum mechanical calculations, J. Comp. Chem. 24 (2003) 1999–2012.
[28] M.S.R. Shell, R. Ritterson, K.A. Dill, A test on peptide stability of Amber force fields with implicit solvation, J. Phys. Chem. B 12 (2008) 6878–6886.
[29] N. Homeyer, A.H. Horn, H. Lanig, H. Sticht, AMBER force-field parameters for phosphorylated amino acids in different protonation states: phosphoserine, phosphothreonine, phosphotyrosine, and phosphohistidine, J. Mol. Model. 12 (2006) 281–289.
[30] W.L. Jorgensen, J. Chandrasekhar, J.D. Madura, R.W. Impey, M.L. Klein, Comparison of simple potential functions for simulating liquid water, J. Chem. Phys. 79 (1983) 926–935.
[31] G. Bussi, D. Donadio, M. Parrinello, Canonical sampling through velocity rescaling, J. Chem. Phys. 126 (2007) 014101.
[32] T. Darden, D. York, L. Pedersen, An N log(N) method for Ewald sums in large systems, J. Chem. Phys. 98 (1993) 10089–10092.
[33] J.C. Ryckaert, G. Ciccotti, H.J.C. Berendsen, Numerical integration of the Cartesian equation of motion of a system with constraints; molecular dynamics of n-alkanes, J. Comp. Chem. 23 (1977) 327–341.
[34] K. Lindorff-Larsen, S. Piana, K. Palmo, P. Maragakis, J.L. Klepeis, R.O. Dror, D.E. Shaw, Improved side-chain torsion potentials for the Amber ff99SB protein force field, Proteins 78 (2010) 1950–1958.
[35] W. Kabsch, C. Sander, Dictionary of protein secondary structure: pattern recognition of hydrogen-bonded and geometrical features, Biopolymers 22 (1983) 2577–2637.
[36] W. Humphrey, A. Dalke, K. Schulten, VMD—visual molecular dynamics, J. Mol. Graph. 14 (1996) 33–38.
[37] C. Haynes, L.M. Iakoucheva, Serine/arginine-rich splicing factors belong to a class of intrinsically disordered proteins, Nucleic Acids Res. 34 (2006) 305–312.
[38] V.N. Uversky, C.J. Oldfield, A.K. Dunker, Showing your ID: intrinsic disorder as an ID for recognition, regulation and cell signaling, J. Mol. Recognit. 18 (2005) 343–384.
[39] E. Nikolakaki, J. Meier, G. Simos, S.D. Georgatos, T. Giannakouros, Mitotic phosphorylation of the lamin B receptor by a serine/arginine kinase and p34(cdc2), J. Biol. Chem. 272 (1997) 6208–6213.
[40] X. Lu, Y. Shi, Q. Lu, Y. Ma, J. Luo, Q. Wang, J. Ji, Q. Jiang, C. Zhang, Requirement for lamin B receptor and its regulation by importin beta and phosphorylation in nuclear envelope assembly during mitotic exit, J. Biol. Chem. 285 (2010) 33281–33293.
[41] J.F. Gui, W.S. Lane, X.D. Fu, A serine kinase regulates intracellular localization of splicing factors in the cell cycle, Nature 369 (1994) 678–682.
[42] S. Yoon, W.J. Welsh, H. Jung, Y.D. Yoo, CSSP2: an improved method for predicting contact-dependent secondary structure propensity, Comput. Biol. Chem. 31 (2007) 373–377.
[43] I. Mylonis, V. Drosou, S. Brancorsini, E. Nikolakaki, P. Sassone-Corsi, T. Giannakouros, Temporal association of protamine 1 with the inner nuclear membrane protein lamin B receptor during spermiogenesis, J. Biol. Chem. 279 (2004) 11626–11631.
[44] M. Takano, Y. Koyama, H. Ito, S. Hoshino, H. Onogi, M. Hagiwara, K. Furukawa, T. Horigome, Regulation of binding of lamin B receptor to chromatin by SR protein kinase and cdc2 kinase in *Xenopus* egg extracts, J. Biol. Chem. 279 (2004) 13265–13271.
[45] M. Takano, M. Takeuchi, H. Ito, K. Furukawa, K. Sugimoto, S. Omata, T. Horigome, The binding of lamin B receptor to chromatin is regulated by phosphorylation in the RS region, Eur. J. Biochem. 269 (2002) 943–953.
[46] H. Polioudaki, N. Kourmouli, V. Drosou, A. Bakou, P.A. Theodoropoulos, P.B. Singh, T. Giannakouros, S.D. Georgatos, Histones H3/H4 form a tight complex with the inner nuclear membrane protein LBR and heterochromatin protein 1, EMBO Rep. 2 (2001) 920–925.